ACS SENSORS

Article

Cite This: ACS Sens. 2019, 4, 2922−2929

pubs.acs.org/acssensors

Ultrasensitive Chemiluminescence Biosensor for Nuclease and Bacterial Determination Based on Hemin-Encapsulated Mesoporous Silica Nanoparticles

Zefeng Gu,[†] Anchen Fu,[†] Li Ye,[§] Kudelaidi Kuerban,[§] Yi Wang,[‡] and Zhijuan Cao*[,†]

[†]Minhang Hospital & Department of Pharmaceutical Analysis at School of Pharmacy, Fudan University, Shanghai 201199, P. R. China

[‡]Center for Advanced Low-dimension Materials, State Key Laboratory for Modification of Chemical Fibers and Polymer Materials, College of Chemistry, Chemical Engineering and Biotechnology, College of Materials Science and Engineering, Donghua University, Shanghai 201620, P. R. China

[§]Department of Microbiological and Biochemical Pharmacy at School of Pharmacy, Fudan University, Shanghai 201203, P. R. China

Supporting Information

ABSTRACT: Bacterial determination, emerging as a critical step in the understanding of increasingly serious bacterial contaminations, remains a major challenge. Herein, a novel chemiluminescence biosensor was exploited for the ultrasensitive determination of nuclease activity and bacteria, in which, hemin, the chemiluminescent (CL) tag molecule was encapsulated into ordered mesopores of mesoporous silica nanoparticles with a specific DNA gate. The capped DNA could be specifically switched upon exposure to the DNA nuclease or bacterial lysate and allowed for an increased release of the encapsulated hemin, which therefore resulted in an obviously enhanced CL signal for the luminol−H_2O_2 system. Attributed to this unique behavior with the linear or sigmoidal relationship between CL intensity and DNA nuclease or bacterial concentration, the as-prepared CL biosensor could detect S1 nuclease activity in the concentration range 0.01−10.0 U with a detection limit of 0.1 mU, and *Escherichia coli* O157:H7 (*E. coli*) or *Staphylococcus aureus* (*S. aureus*) in the concentration ranges 10^1 to 10^9 cfu mL^{-1}. The detection limit of *E. coli* and *S. aureus* was calculated to be 3.0 and 2.5 cfu mL^{-1}, respectively, which was comparable or even better than that of previous studies. Thus, this detection method could achieve detectable levels without cell enrichment overnight. Moreover, the proposed biosensing system could be conducted in the homogeneous solution without separation and washing, greatly improving the reaction efficiency and simplifying the procedure. As expected, the novel CL biosensor promised a great potential for simple and convenient detection of nuclease and bacteria in fields such as food bacterial contamination, pharmaceuticals, and clinical analysis.

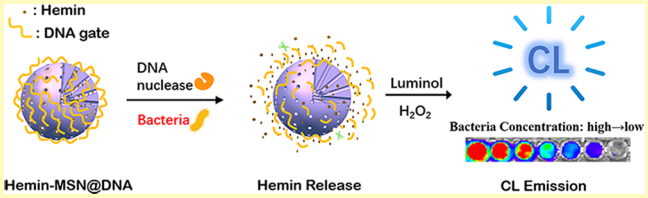

KEYWORDS: *encapsulated hemin, mesoporous silica nanoparticles, nuclease, bacteria, chemiluminescence*

Pathogen infection, such as the most frequently occurred contaminations of air, food, drinking water, and human contacts,[1,2] has been considered as a severe threat to global health.[3] To address this issue, various methods, including plate-counting technique,[4] polymerase chain reaction,[5] enzyme-linked immuno-sorbent assay,[6,7] and gene technique,[8−10] have been developed for pathogenic microbial detection. However, complicated and time-consuming manipulations with a valuable apparatus and low sensitivity are often involved, which greatly depress their practical applications. Comparatively, chemiluminescence (CL) relies on illumination produced by chemical reactions of trace analysts, which can be exempted from the excitation light source and therefore avoid interference from light scattering.[11] As a result, CL possesses simple instrumentation and operation, wide calibration ranges, and suitability for miniaturization,[12,13] offering a great potential for the determination of pathogenic microorganisms.[14] Classically, luminol-based CL reaction coupling of hydrogen peroxide (H_2O_2) and other oxidations is the main illuminated medium because of its inexpensiveness and high sensibility. It was known that the original CL signal is very weak without enhancement. Therefore, various reagents, including metal ions, metal oxides, nanoparticles and enzymes, have been widely used to magnify the CL signal.[15−17] Nevertheless, to specify the magnified CL signal with the targeted analyst, stimuli-responsive biosensing systems need to be carefully established, which consequently request versatile nanostructured materials such as mesoporous materials (silica, carbon, and metal oxides), liposomes, and polymers.[18,19] Among these materials, mesoporous silica nanoparticles (MSNs) have drawn great attention because of their unique pore structure with large pore volumes and surface areas and good biocompati-

Received: July 12, 2019
Accepted: November 1, 2019
Published: November 1, 2019

DOI: 10.1021/acssensors.9b01303
ACS Sens. 2019, 4, 2922−2929

bility. In particular, MSNs can encapsulate numerous guest molecules to promote their performances in bioanalysis and imaging via different stimuli, including pH or magnetic change, reduction, light, enzymes, and dual-responsive factors,[20−23] showing potential promise for constructing sensitive CL systems. However, engineering the stimuli-responsive CL systems with specific DNA molecules for sensitive nuclease activity or bacterial determination in the real samples is still an urgent challenge.

In this work, a novel material, hemin−MSN@DNA, was designed and prepared as an ultrasensitive chemiluminescence probe for nuclease activity and bacterial determination. For that, the CL enhancement tag (hemin) was encapsulated into the pores of MSNs and then capped with the designed DNA via electrostatic interaction. With the presence of DNA nuclease (here, S1 nuclease, an important indicator related to the disease state, was used as a model),[24] the capped DNA would be hydrolyzed into 5′-phosphomononucleotide or 5′-phospho-oligonucleotides, which thus trigger the hemin release to enhance the CL emission greatly for nuclease activity quantification. Moreover, attributing to the sensitive stimuli response of specific DNA gate to DNA nuclease, the nuclease derived from bacteria can also digest DNA gate to trigger CL enhancement. Thus, this biosensing method can also be extended to detect the bacterial contamination in milk and drinking water, which provides a robust alternation for food safety monitoring and clinical applications.

EXPERIMENTAL SECTION

Chemicals and Reagents. All the oligonucleotides used in this work were synthesized by KareBay Biochem, Inc. (Ningbo, China) and purified by high-performance liquid chromatography. The sequences of the DNA oligonucleotides are listed in Table S1. The stock solutions of DNA were obtained by dissolving DNA in sterile deionized water. Hydrogen peroxide (H_2O_2), sodium hydroxide (NaOH), 3-amino-propyltriethoxysilane (APTES), cetyltrimethyl ammonium bromide (CTAB), tetraethyloxysilane (TEOS), ammonium nitrate (NH_4NO_3), methanol, and ethanol were obtained from Sinopharm Chemical Reagent Co., Ltd. (Shanghai, China). Luminol (3-aminophthalhydrazide), thrombin, and hemin were purchased from Sigma-Aldrich (St. Louis, MO). DNA ladder, 10× loading buffer, Exo I, Exo III, DNase I, and λexo were purchased from the Takara Biotechnology Co., Ltd. (Dalian, China). Bovine serum albumin (BSA) was bought from Sino-American Biotechnology Co. (Shanghai, China). All the chemicals were of analytical grade. All the stock and buffer solutions were prepared in distilled water purified by using a Milli-Q water purification system (Millipore Corp., Bedford, MA) with an electrical resistance of 18.2 MΩ at 25 °C. Phosphate-buffered saline (PBS, 137 mM NaCl, 2.68 mM KCl, 10.1 mM Na_2HPO_4, 1.76 mM KH_2PO_4, pH 7.4) and PBS−dimethyl sulfoxide (DMSO) buffer (1:1) were used to prepare hemin stock solution. PBS and PBS-TW (0.05% Tween) were employed as the reaction and washing buffer in this study, respectively. *Escherichia coli* O157:H7 (*E. coli*, ATCC 35150) and *Staphylococcus aureus* (*S. aureus*, ATCC 25923) were cultured in Luria−Bertani (LB) broth (Thermo Fisher Scientific, USA). The CellTiter-Glo luminescent cell viability assay kit was bought from Promega Corporation (Wisconsin, USA).

Apparatus. CL measurements were performed with a BPCL ultraweak luminescence analyzer (Institute of Biophysics, Chinese Academy of Sciences, Beijing, China). The CL signal was measured in a glass cuvette. All the CL measurements were performed at room temperature (25 °C). UV absorption was measured by using UV-2900 (Hitachi, Japan). The reaction was conducted in Thermo Scientific MaxQ Shakers. Heraeus Pico 17 Microcentrifuge (Thermo Scientific, USA) was employed for separation and purification of nanomaterials. Particle sizes of MSNs were characterized by using a Nano-ZS (Malvern, UK). High-resolution transmission electron microscopy (TEM) and dark field scanning TEM (STEM) with energy dispersive X-ray spectroscopy (EDXS-mapping) were performed on JEM-2100F instruments with an acceleration voltage of 200 kV. The samples were dispersed as slurry in PBS and dried on a Cu grid before the measurement. Adenosine 5′-triphosphate (ATP)-based luminescent signal was recorded by using Fluroskan Ascent FL (Thermo Electron Corporation, USA). Luminescence images were obtained on the Xenogen IVIS Spectrum imaging system (Caliper Life Sciences, USA).

Preparation of Aminated MSNs. Aminated MSNs were synthesized via surfactant-assisted self-assembly. Typically, 100 mg of CTAB was first dissolved in 48 mL of aqueous NaOH (14.5 mM) via vigorous stirring at 80 °C. Then, 500 mL of TEOS and 100 μL of APTES−ethanol solution (1/4, v/v) were successively added, and the solution was stirred for about 2 h. After that, the solid product was obtained via centrifugation and washing. To remove the surfactants from the pores, the obtained nanoparticles were repeatedly refluxed in NH_4NO_3−methanol solution (2 mg mL^{-1}). Finally, aminated MSNs were recovered by freeze-drying and characterized by TEM and Nano-ZS Zetasizer (Malvern, UK).

Preparation of Hemin-Loading MSNs Capped with the DNA Gate (Hemin−MSN@DNA). Hemin−MSNs was synthesized from the as-prepared aminated MSNs and hemin stock solution. Initially, 1 mg of aminated MSNs was ultrasonically dispersed in 500 μL of PBS buffer to obtain a uniform suspension. Then, 200 μL of hemin stock solution (1.2 mM) in PBS−DMSO (1:1) was added dropwise into the suspension of aminated MSNs under magnetic stirring. The resultant mixture was stirred at room temperature for 10 min until it became clear and dark brown. The strong preferential interaction between the hemin molecules and the silica walls resulted in the significant concentration gradients within the pores, and a noticeable amount of hemin molecules could be loaded into MSNs to form hemin−MSNs. Subsequently, 300 μL of DNA (2 nmol) was dispersed directly into the above mixture and incubated at 37 °C for 3 h. During the procession, the pores of the aminated MSNs could be sealed by the DNA gate to be hemin−MSN@DNA based on the electrostatic interaction between electropositive MSNs and electronegative DNA. The hemin−MSN@DNA was collected by centrifugation (10 000 rpm, 3 min) and washed with PBS-TW 3 times to remove the free and surface-absorbed hemin and DNA strands. The obtained brown precipitate was resuspended by ultrasonication for a few seconds and kept in 250 μL of PBS for the subsequent experiments. To study hemin−MSN@DNA stability, the CL signal of its stock solution was detected at 0, 2, 4, 6, 8, and 24 h. The CL signal of totally leached hemin molecules was used as the control.

Gel Electrophoresis. To confirm the cleavage of the DNA probe by nucleases and bacterial lysate, a gel-based degradation assay was performed. To prepare 8.0% polyacrylamide gel, 8 mL of 30% acrylamide (29:1) solution was mixed with 6 mL of 5× Tris-borate buffer (TBE, 0.2 M Tris base, 0.22 M boric acid, 6.3 mM ethylenediaminetetraacetic acid, pH 8.0), 16 mL of pure water, 300 μL of 10% ammonium persulfate, and 18 μL of tetramethylethylenediamine, sequentially. Here, 1× TBE was used as running buffer. For each assay sample, 1 pmol DNA probe was mixed with 2 U of various DNA nucleases, BSA (1 mg mL^{-1}), and designed concentrations of *E. coli* lysate, in the final volume of 10 μL, and the mixture was allowed to react at room temperature for 1 h. After that, 10 μL of the above reaction solution was mixed with 1 μL of 10× loading buffer and subjected to electrophoresis on the 8.0% polyacrylamide gel. A DNA ladder with molecular weight markers ranging from 20 to 500 bp was used. Polyacrylamide gels were run at 120 V for 40 min and stained for 20 min in 3× GelRed solution (Biotium, USA), followed by observation of electrophoresis bands with FluorChem SP.

Bacterial Culture Samples. *E. coli* was grown overnight (20 h) in 50 mL of LB broth under 200 rpm at 37 °C. The concentration of *E. coli* was measured by using a Nano-ZS particle size instrument to be 1.34×10^9 cfu mL^{-1}. Similarly, *S. aureus* was cultured in LB broth and measured to be 1.1×10^9 cfu mL^{-1}. The overnight cultures were then centrifuged at 7000*g* for 2 min, washed 2 times with PBS, and

DOI: 10.1021/acssensors.9b01303
ACS Sens. 2019, 4, 2922−2929

resuspended in PBS buffer. In addition, we prepared some samples to investigate the bacterial contaminations in drinking water and skim milk. Drinking water was obtained from the drinking water fountain at Fudan University. Skim milk was purchased in a local supermarket. We prepared 10 samples, including drinking water (a) and skim milk (f) stored at 4 °C. Water and milk were spiked with bacteria (6.7×10^6 cfu mL^{-1}) as the samples b and g. Water and milk were sealed and incubated at 37 °C overnight (c and h). Water and milk were inoculated by *E. coli* and incubated at 37 °C overnight (d and i). Water and milk exposed in the air were set as samples e and j. All these samples were then centrifuged at 7000*g* for 2 min, washed 2 times with PBS, and resuspended in PBS buffer. Moreover, several aqueous samples were collected for the comparison of our protocol and the commercial one (ATP-based bioluminescence method).

Detection of S1 Nuclease. In a typical experiment, 10 μL of the as-prepared hemin−MSN@DNA and 10 μL of different concentrations of S1 nuclease in PBS were mixed and gently shaken in the incubator for 1 h at 37 °C. Finally, 20 μL of the above solution was transferred to a glass tube (14 × 40 mm) and mixed with 10 μL of luminol (10 μM) and 110 μL of PBS. When 10 μL of H_2O_2 (10 μM) was added, the CL signal of the mixture was immediately monitored by using the BPCL ultraweak luminescence analyzer.

Detection of DNA Nuclease Activity in Bacterial Lysate and Water/Milk Samples. Ten microliters of bacterial samples was treated in 90 μL of bacterial lysis buffer (Thermo Fisher Scientific, USA) at room temperature for 20 s, which was then serially diluted to desired concentrations of 10^1, 10^2, 10^3, 10^4, 10^5, 10^6, 10^7, 10^8, and 10^9 cfu mL^{-1} in the reaction buffer for the calibration curve. Similarly, 10 μL of water, milk, or other aqueous samples was treated in 90 μL of bacterial lysis buffer at room temperature for 20 s, and 10-fold diluted before detection. Then, 10 μL of each sample was added into the as-prepared hemin−MSN@DNA and gently shaken for 1 h at 37 °C. The resultant mixture was transferred to a glass tube. One hundred and ten microliters of PBS and 10 μL of luminol were added and mixed thoroughly. Finally, the CL signal was immediately monitored as 10 μL of H_2O_2 was added.

Luminescence Image for the Detection of Bacteria. Ten microliters of *E. coli* bacterial samples (10^4, 10^5, 10^6, 10^7, 10^8, and 10^9 cfu mL^{-1}) and spiked samples (5.5×10^5, 5.5×10^6, and 5.5×10^7 cfu mL^{-1}) were added into the as-prepared hemin−MSN@DNA and gently shaken for 1 h at 37 °C. The resultant mixture was transferred to a black 96-well plate. One hundred and ten microliters of PBS and 10 μL of luminol (1 mM) were added and mixed thoroughly. Finally, as 10 μL of H_2O_2 (1 mM) was added, the luminescent signal was immediately measured by using the Xenogen IVIS Spectrum imaging system.

Bacterial Determination Using the ATP-Based Bioluminescence Method. To compare our CL-based method with a commercial one for bacterial determination, the ATP-based bioluminescence method was performed on several concentrations of bacteria and other aqueous samples, including different concentrations of bacterial solutions (10^1 to 10^9 cfu mL^{-1}) and samples, including water, milk, watermelon, or pear juice. The bacterial measurements using the ATP-based system were performed by following the commercial manual (CellTiter-Glo luminescent cell viability assay kit, Promega, USA). One hundred microliters of bacterial or other aqueous samples was placed in each well of an opaque-walled multiwell plate and equilibrated for approximately 30 min at room temperature. Then, an equal volume of the CellTiter-Glo reagent was added into the well. The resultant mixture was mixed for 2 min on an orbital shaker and incubated for 10 min. Finally, the luminescent signal was recorded by using a Fluroskan Ascent FL (Thermo Electron Corporation, USA).

RESULTS AND DISCUSSION

Design of the Stimuli-Responsive CL Biosensor Based on Hemin−MSN@DNA. The MSN-based stimuli-responsive CL biosensor for the determination of DNA nuclease and pathogen microorganisms is illustrated in Scheme 1. Aminated

Scheme 1. Schematic Presentation of the Stimuli-Responsive CL Platform for DNA Nuclease and Bacterial Detection

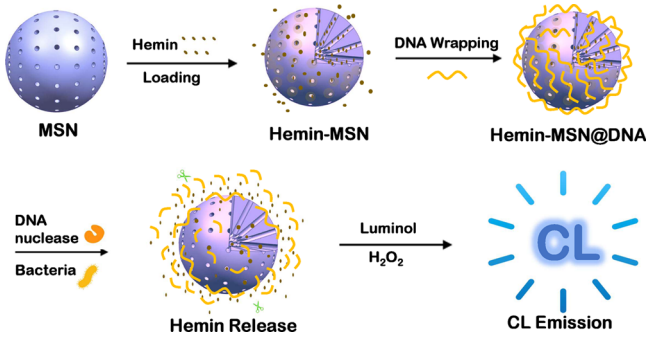

MSNs were first synthesized via surfactant-assisted self-assembly, which were homogeneously dispersed near-spherical nanoparticles with a diameter of 125 ± 15 nm (Figure 1). These nanoparticles possessed highly ordered and fitly distributed mesopores with a pore size of ∼2.7 nm as observed from the magnified TEM images (Figure 1A,B). After encapsulation of hemin via pore adsorption and then gating by DNA via electrostatic interaction, the obtained hemin−MSN@DNA hybrids remained as near-spherical nanoparticles with a little larger size. Differently, the surface of hemin−MSN@DNA was much rougher than that of pristine-aminated MSNs, and the mesopores were hardly observed. It suggested that hemin was loaded into the mesopores and the surface of aminated MSNs was coated by DNA. To further prove this, EDX-pattern and EDX-mapping images were also acquired on the hemin−MSN@DNA nanoparticles, which demonstrated obvious Fe and P signals within the silica matrix, corresponding to the encapsulated hemin and the DNA gate. Furthermore, only a little larger particle size for hemin−MSN@DNA than that for MSN measured by TEM (Figure 1C−J) due to surface modification and hydrophilization validated this special coating (Figure S1). Moreover, this phenomenon also confirmed the good water dispersity of hemin−MSN@DNA with good stability within 24 h (Figure S2). All these results revealed that animated MSNs with ordered mesopores were synthesized, and active hemin molecules could be easily loaded into the mesopores which were then well gated by DNA. Much interestingly, the sealed mesopores of hemin−MSN@DNA could be conveniently opened upon the exposure to DNA nuclease or bacterial lysate because of the specific degradation performance on the DNA gate. This manner could induce a release of hemin molecules into the solution, thus triggering the CL reaction between luminol and H_2O_2 to enhance the CL emission. As expected, the CL emission was linearly enhanced with primary pore triggers (DNA nuclease and pathogen microorganisms). Therefore, a sensitive CL biosensor based on an interesting configuration, a specific DNA gate together with the highly sensitive and strong chemiluminescent enhancer reagent, would be prepared, which could be exploited for sensing nuclease activity and bacterial contamination.

Optimization of Parameters. To optimize the biosensing performance, the DNA configuration was investigated for the optimal pore sealing. CL intensity was detected before and after the reaction between S1 nuclease with three hemin−MSN@DNA materials with three different DNA gates. As shown in Figure 2A, a special-structured DNA, SSD-1

DOI: 10.1021/acssensors.9b01303
ACS Sens. 2019, 4, 2922−2929

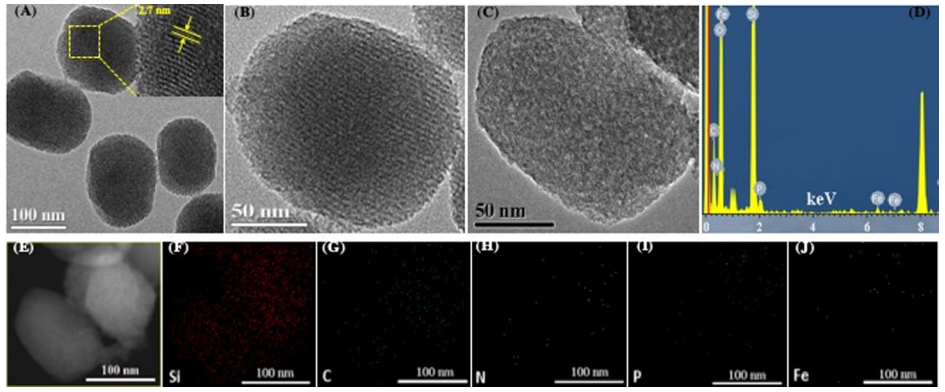

Figure 1. TEM images of MSNs (A,B) and hemin−MSN@DNA (C). The inset in (A) showed the mesopores of MSNs. The EDX-pattern (D) and STEM image (E) of hemin−MSN@DNA. EDX-mapping images (F−J) of hemin−MSN@DNA.

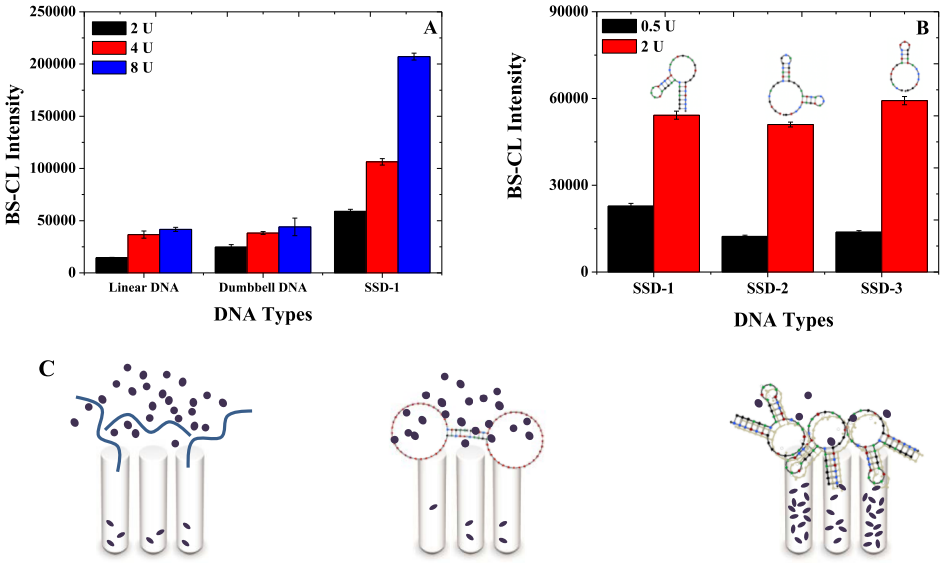

Figure 2. BS-CL intensity vs (A) different types of DNA gates and (B) three special-structured DNA gates, and (C) the possible structures of gated DNA and its interaction with MSNs (from left to right: linear, dumbbell, and special-structured DNA gates). (A) Black, red, and blue lines correspond to 2, 4, and 8 U S1 nuclease, respectively. (B) Black and red lines correspond to 0.5 and 2 U S1 nuclease, respectively. All the DNA gates were set at 2 μM. Measurements were performed by using 10 μL of the as-prepared hemin−MSN@DNA, 10 μL of luminol (10 μM), 10 μL of H_2O_2 (10 μM), and 110 μL of PBS. Data were presented as mean ± SD (n = 3). BS-CL intensity denotes background-subtracted chemiluminescent signal.

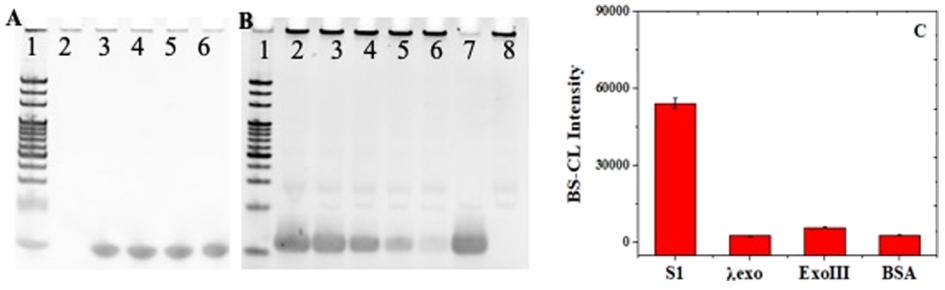

Figure 3. Nondenatured polyacrylamide gel electrophoresis images (A,B) and the CL signal with different nucleases and protein (C). A1: DNA marker (20 to 500 bp increments), A2: SSD-1 + S1, A3: SSD-1, A4: SSD-1 + Exo III, A5: SSD-1 + λexo, and A6: SSD-1 + BSA (1 mg mL^{-1}). B1: DNA marker, B2: SSD-1 + bacterial lysate (1 × 10^1 cfu mL^{-1}), B3: SSD-1 + bacterial lysate (1 × 10^3 cfu mL^{-1}), B4: SSD-1 + bacterial lysate (1 × 10^5 cfu mL^{-1}), B5: SSD-1 + bacterial lysate (1 × 10^7 cfu mL^{-1}), B6: SSD-1 + bacterial lysate (1 × 10^9 cfu mL^{-1}), B7: SSD-1 with lysis buffer, and B8: bacterial lysate. (C) The concentration of S1, Exo III, and λexo was set at 2 U, while BSA was 1 mg mL^{-1}. All the samples were prepared with PBS. The concentration of S1, Exo III, and λexo was set at 2 U. CL measurements were performed by using 10 μL of the as-prepared hemin−MSN@DNA, 10 μL of luminol (10 μM), 10 μL of H_2O_2 (10 μM), and 110 μL of PBS. Data were presented as mean ± SD (n = 3). BS-CL intensity denotes background-subtracted chemiluminescent signal.

DOI: 10.1021/acssensors.9b01303
ACS Sens. 2019, 4, 2922−2929

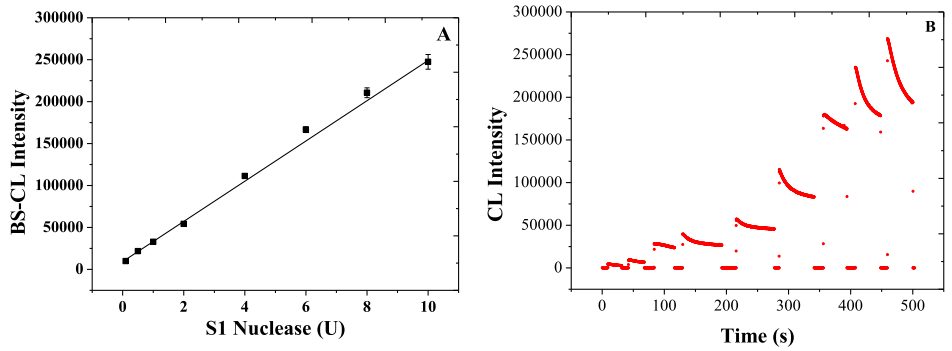

Figure 4. BS-CL intensity vs concentrations of S1 nuclease (A) and CL intensity plot vs times (B). (A) Each dot was corresponding to different S1 nuclease concentrations; (B) each kinetic curve was corresponding to different S1 nuclease concentrations. From left to right, S1 nuclease: 0, 0.1, 0.5, 1, 2, 4, 6, 8, and 10 U. Measurements were performed using 10 μL of hemin−MSN@DNA, 10 μL of luminol (10 μM), 10 μL of H_2O_2 (10 μM), and 110 μL of PBS. Data were presented as mean ± SD (n = 3). BS-CL intensity denotes background-subtracted chemiluminescent signal.

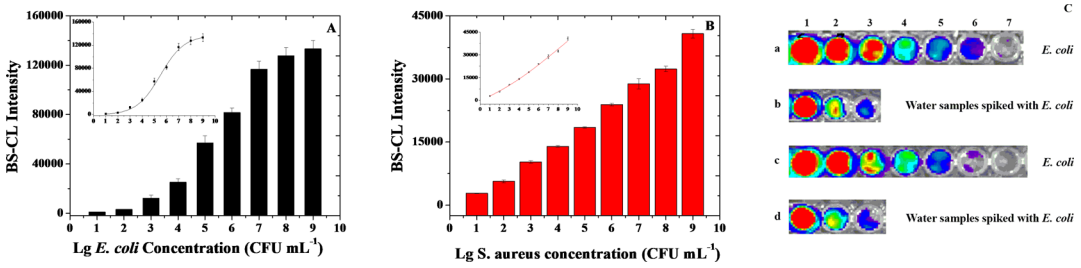

Figure 5. BS-CL intensity vs different concentrations of *E. coli* bacteria (A) and *S. aureus* (B) and luminescence images for different concentrations of *E. coli* bacteria (C). (A)-inset: Calibration curve for *E. coli* concentration (cfu mL^{-1}). (B)-inset: Calibration curve for *S. aureus* concentration (cfu mL^{-1}). Measurements were performed using 10 μL of hemin−MSN@DNA, 10 μL of luminol [1 mM for (C) and 10 μM for (A,B)], 10 μL of H_2O_2 [1 mM for (C) and 10 μM for (A,B)], and 110 μL of PBS. Data were presented as mean ± SD (n = 3). BS-CL intensity denotes background-subtracted chemiluminescent signal. (C) a1−a7: *E. coli* bacterial concentrations of 10^9, 10^8, 10^7, 10^6, 10^5, 10^4, and 0 cfu mL^{-1}, respectively. b1−b3: Water samples spiked with different concentrations of *E. coli* bacterial (5.5×10^7, 5.5×10^6, and 5.5×10^5 cfu mL^{-1}, respectively). c1−c7: Replicates for a1−a7. d1−d3: Replicates for b1−b3.

(aptamer for cocaine), contributed the strongest CL enhancement as compared with linear (T40) or dumbbell DNA (a strand with two 30-mer loops and a nicked 10 bp stem). To confirm the structure effect, we investigated another two special-structured DNAs, that is, SSD-2 (aptamer for PDGF) and SSD-3 (aptamer for thrombin), as the gate. As shown in Figure 2B, all the SSD DNA gates contributed similar CL enhancement with the increasing S1 nuclease. Based on that, we assumed that the random coiled aptamer DNAs, with proper conformation and electrostatic binding force, were the better gates for the pores on the surface of MSNs than the linear or well-folded dumbbell DNAs.[20,25−27] Therefore, we deduced the possible mechanism of gated DNA and its interaction with MSNs (as shown in Figure 2C). Following that, other conditions were investigated for this method. As exhibited in Figure S3, PBS−DMSO (1:1) with 3 h reaction time mediated the optimal hemin encapsulation and thus contributed to the most remarkable CL enhancement in this biosensing system. Comparatively, pure PBS or DMSO would depress the biosensing performances, possibly because of the improper hemin solubility-caused low loading efficiency in these mediums. As demonstrated in Figure S4, 1.2 mM hemin loaded into 2 mg mL^{-1} MSNs gated with 2 μM SSD-1 produced appreciable CL enhancement, where a comparatively low CL background and high sensitivity were obtained, possibly attributed to good hemin-loading efficiency and DNA wrapping which was suitable to be digested by S1 nuclease or bacterial lysate. Under the optimal condition, the hemin loading efficiency and the wrapping efficiency of the DNA gate were determined to be 58.8 ± 0.8 and 62.7 ± 1.7% based on CL and UV absorption detection, respectively. The nuclease cleaving kinetic curve was investigated to find out the optimal incubation time. As seen in Figure S5, 60 min was chosen for the experiment.

Tests on Feasibility of DNA Nuclease and Bacterial Detection. Prior to the detection of nuclease activity and bacteria by using the CL platform, the feasibility of this biosensor was tested by gel electrophoresis. As shown in Figure 3A, gel images of DNA probes were obtained, which were incubated with various nucleases, proteins, and *E. coli* bacterial lysates. Among them, the SSD-1 probe was used as the control (lane A3). Lanes A2, A4, A5, and A6 were corresponding to the DNA probe incubated with S1 nuclease (endonuclease), Exo III, λexo (exonuclease), and BSA (protein), respectively. According to that, only S1 nuclease could digest SSD-1 thoroughly, which were also confirmed by the CL measurement (Figure 3C). Furthermore, we detected other nucleases, including DNase I and Exo I, which showed the same effect as S1 nuclease and could degrade SSD-1 (for data see Figure S6). Therefore, we deduced that DNA nucleases in bacteria might also digest the DNA probe to induce CL enhancement. Then, bacterial lysate from *E. coli* was studied to testify the assumption. As shown in Figure 3B, lane B7 was the negative control, which demonstrated that lysis buffer alone without bacteria could not digest SSD-1. Moreover, lane B8 (the second negative control) was *E. coli* bacterial lysate without SSD-1, which showed that *E. coli* bacterial lysate contained some macromolecules (the top dark band at the loading

DOI: 10.1021/acssensors.9b01303
ACS Sens. 2019, 4, 2922−2929

Table 1. Analysis of Bacterial Contamination in Drinking Water and Milk

samples	spiked (cfu mL^{-1})	measured (cfu mL^{-1})	RSD (%)	recovery (%)	sample concentration (cfu mL^{-1})
a					
b	6.700×10^6	6.068×10^6	1.10	90.57	
c					
d		6.782×10^5	2.39		6.782×10^7
e		0.450×10^1	13.5		450
f		3.380×10^1	2.40		3.380×10^3
g	6.700×10^6	6.579×10^6	1.67	98.20	
h		4.066×10^5	2.34		4.066×10^7
i		4.699×10^7	2.79		4.699×10^9
j		1.100×10^3	4.91		1.100×10^5

position in lane B2−B6 and B8). However, these macromolecules (e.g.,proteins) did not influence the band of the SSD-1 probe. Finally, the bands of SSD-1 shoaled gradually with the increase of *E. coli* concentration after incubating with bacterial lysate (with different concentrations of *E. coli*, lanes B2−B6). The result indicated obviously that the DNA probe could be degraded by DNA nucleases in *E. coli* bacterial lysate, which was confirmed by further CL measurements (see Figure 5B).

Determination of S1 Nuclease Activity and Bacterial Contamination. Under the optimal conditions, the S1 nuclease-dependent CL signal has been quantitatively investigated by using this CL platform. The background-subtracted CL (BS-CL) signal (I) increased linearly with the concentration of S1 nuclease in the range 0.1−10 U (I = 24 581 [S1] + 8800, R^2 = 0.996), where I is the corresponding BS-CL intensity in different concentrations of S1 (Figure 4A). The detection limit of S1 was calculated to be 0.1 mU with threefold standard deviation of the background signal (3σ). As shown in Figure 4B, CL intensity was recorded for each concentration. Nevertheless, in order to evaluate the practical potential of this strategy, the possible application on the determination of DNA nuclease in bacterial lysate was studied. To determine bacteria, the concentration-dependent CL signal was measured from 1.0×10^1 to 1.0×10^9 cfu mL^{-1} *E. coli* or *S. aureus* bacteria. As shown in Figure 5A,B, the CL signal gradually increased with increasing *E. coli* concentrations. A calibration graph showed a good correlation between the CL intensity and logarithm of bacterial concentrations, as represented by $I_E = 136\,987.0 - 137\,454.2/[1 + \exp((C_E - 5.501)/0.980)]$ (R^2 = 0.9956) for *E. coli* and $I_S = 90\,327.2 - 106\,530.8/[1 + \exp((C_S - 8.601)/4.976)]$ (R^2 = 0.9985) for *S. aureus*, where I_E and I_S are the CL intensity subtracted from the background (BS-CL intensity) for *E. coli* and *S. aureus*, respectively. C_E and C_S are the bacterial concentration of *E. coli* and *S. aureus*, respectively. The detection limit was calculated to be 3.0 cfu mL^{-1} for *E. coli* and 2.5 cfu mL^{-1} for *S. aureus* based on threefold standard deviation of the background signal (3σ), which was comparable or even better than that of previous studies (listed in Table S2). In addition, as shown in Figure 5C, the luminescent image was detected twice with different *E. coli* bacterial standard concentrations and spiked water samples.

To evaluate the specificity for the detection of enzyme activity, dry heating was applied in this study as a simple and economical sterilization method. To prepare inactive nuclease and bacterial samples, 2 U S1 nuclease, 10^4 cfu mL^{-1} *E. coli*, and 10^4 cfu mL^{-1} *S. aureus* was heated at 100 °C for 30 min, which was treated in lysis buffer and detected according to the procedure in the revised manuscript. As demonstrated in Figure S7, the live nuclease and bacteria showed a significantly higher CL enhancement than the signal observed after heating. It meant that the activity of nuclease or enzyme activity in bacteria played an important role for this measurement.

The safety of drinking water is a critical health issue, and milk is often associated with the foodborne outbreaks.[28] Thus, we applied the established stimuli-responsive CL detection in real drinking water and skim milk samples. As shown in Table 1, drinking water, even incubated overnight at 37 °C, was detected to have no obvious contamination (sample a and c). However, if we inoculated *E. coli* to the drinking water, we could detect the bacterial concentration to be 6.782×10^7 (sample d) after incubation overnight. Correspondingly, it was determined to be 3.380×10^3 cfu mL^{-1} in packaged milk (sample f) and sharply improved to be 4.066×10^7 cfu mL^{-1} after being incubated at the same condition as *E. coli* (sample h). After the *E. coli* inoculation into milk sample, the bacterial concentration was found to be 4.699×10^9 cfu mL^{-1} (sample i). It was suggested that *E. coli* could propagate in both water and milk. In addition, milk might be the better matrix for bacterial propagation. Moreover, the quantitative recoveries of spiked water and milk sample were demonstrated to be 90.57 and 98.20%, respectively (sample b and g). It was noteworthy that the water and milk samples exposed in the air were also detected to be 450 and 1.100×10^5 cfu mL^{-1} without cell enrichment overnight (sample e and j), which confirmed that our new method could be applied in real food sample analysis conveniently.

Furthermore, the ATP-based bioluminescence technology was used to verify our measurement. As shown in Figure S8, the lowest *E. coli* concentration we could detect was demonstrated to be 10^6 cfu mL^{-1} by using the ATP-based method. Then, we compared the detection of different samples between that method and our protocol. As seen in Figure S9, the signal pattern of bacterial detection between the two methods was similar in each location, indicating that our proposed method was comparable to a conventional ATP-based method. Moreover, the sensitivity of our method was much better than the ATP-based one.

CONCLUSIONS

In conclusion, an ultrasensitive CL biosensor, where CL tag molecule-hemin was well sealed into ordered mesopores of MSNs by a specific DNA gate, was prepared. Owing to the hemin-mediated CL enhancement and the optimal matching of special-structured DNA gate with columned pores of MSNs and the sensitive stimuli responsiveness, the as-prepared biosensor can achieve the detection of S1 nuclease, *E. coli*,

DOI: 10.1021/acssensors.9b01303
ACS Sens. 2019, 4, 2922−2929

and *S. aureus* with the low detection limit of 0.1 mU, 3.0, and 2.5 cfu mL^{-1}, respectively, which are comparable or superior to those of many previous studies. Consequently, the practical bacterial contamination detection in milk and drinking water was simply realized. This method is cost-effective without complex equipment or reagents and easy to prepare without tedious separation procedures. Therefore, it provides an alternative to monitor the diseases associated with the abnormal level of DNA nuclease and food or environmental contamination. Especially, attributed to that many aptameric DNA special secondary structures, this method is promising to be extended to the detection of various targets with aptamers.

■ ASSOCIATED CONTENT

Supporting Information

The Supporting Information is available free of charge on the ACS Publications website at DOI: 10.1021/acssensors.9b01303.

Table of DNA sequences, figures and texts for material DLS data, stability test, parameter optimization, and some verification experiments and comparison experiments (PDF)

■ AUTHOR INFORMATION

Corresponding Author

*E-mail: zjcao@fudan.edu.cn (Z.C.).

ORCID

Li Ye: 0000-0001-5303-2549

Yi Wang: 0000-0003-3345-4319

Zhijuan Cao: 0000-0002-0926-733X

Notes

The authors declare no competing financial interest.

■ ACKNOWLEDGMENTS

The authors are grateful to the projects of the National Natural Science Foundation of China (nos. 21505023 and 21675032) and the Fundamental Research Funds for the Central Universities and DHU Distinguished Young Professor Program.

■ REFERENCES

(1) Brecher, M. E.; Hay, S. N. Bacterial contamination of blood Components. *Clin. Microbiol. Rev.* **2005**, *18*, 195−204.

(2) Teengam, P.; Siangproh, W.; Tuantranont, A.; Vilaivan, T.; Chailapakul, O.; Henry, C. S. Electrochemical impedance-based DNA sensor using pyrrolidinyl peptide nucleic acids for tuberculosis detection. *Anal. Chim. Acta.* **2018**, *1044*, 102−109.

(3) Ray, P. C.; Khan, S. A.; Singh, A. K.; Senapati, D.; Fan, Z. Nanomaterials for targeted detection and photothermal killing of bacteria. *Chem. Soc. Rev.* **2012**, *41*, 3193−3209.

(4) Rahman, M.; Kühn, I.; Rahman, M.; Olsson-Liljequist, B.; Möllby, R. Evaluation of a scanner-assisted colorimetric MIC method for susceptibility testing of gram-negative fermentative bacteria. *Appl. Environ. Microbiol.* **2004**, *70*, 2398−2403.

(5) Law, J. W.-F.; Ab Mutalib, N.-S.; Chan, K.-G.; Lee, L.-H. Rapid methods for the detection of foodborne bacterial pathogens: principles, applications, advantages and limitations. *Front. Microbiol.* **2015**, *5*, 770.

(6) Liu, D.; Wang, Z.; Jin, A.; Huang, X.; Sun, X.; Wang, F.; Yan, Q.; Ge, S.; Xia, N.; Niu, G.; Liu, G.; Hight Walker, A. R.; Chen, X. Acetylcholinesterase-catalyzed hydrolysis allows ultrasensitive detection of pathogens with the naked eye. *Angew. Chem., Int. Ed.* **2013**, *52*, 14065−14069.

(7) Hou, Y.-H.; Wang, J.-J.; Jiang, Y.-Z.; Lv, C.; Xia, L.; Hong, S.-L.; Lin, M.; Lin, Y.; Zhang, Z.-L.; Pang, D.-W. A colorimetric and electrochemical immunosensor for point-of-care detection of enterovirus 71. *Biosens. Bioelectron.* **2018**, *99*, 186−192.

(8) Xu, Y.; Wei, Y.; Cheng, N.; Huang, K.; Wang, W.; Zhang, L.; Xu, W.; Luo, Y. Nucleic acid biosensor synthesis of an All-in-One universal blocking linker recombinase polymerase amplification with a peptide nucleic acid-based lateral flow device for ultrasensitive detection of food pathogens. *Anal. Chem.* **2018**, *90*, 708−715.

(9) Lin, X.; Liu, Y.; Deng, J.; Lyu, Y.; Qian, P.; Li, Y.; Wang, S. Multiple advanced logic gates made of DNA-Ag nanocluster and the application for intelligent detection of pathogenic bacterial genes. *Chem. Sci.* **2018**, *9*, 1774−1781.

(10) Tram, K.; Kanda, P.; Salena, B. J.; Huan, S.; Li, Y. Translating bacterial detection by DNAzymes into a litmus test. *Angew. Chem., Int. Ed.* **2014**, *53*, 12799−12802.

(11) Huertas-Pérez, J. F.; Moreno-González, D.; Airado-Rodríguez, D.; Lara, F. J.; García-Campaña, A. M. Advances in the application of chemiluminescence detection in liquid chromatography. *TrAC, Trends Anal. Chem.* **2016**, *75*, 35−48.

(12) Yousefzadeh, A.; Hassanzadeh, J.; Mousavi, S. M. J.; Yousefzadeh, M. Surface molecular imprinting and powerfully enhanced chemiluminescence emission by Cu nanoclusters/MOF composite for detection of tramadol. *Sens. Actuators, B* **2019**, *286*, 154−162.

(13) Suzuki, K.; Nagai, T. Recent progress in expanding the chemiluminescent toolbox for bioimaging. *Curr. Opin. Biotechnol.* **2017**, *48*, 135−141.

(14) Bui, M.-P. N.; Brockgreitens, J.; Abbas, A. Gold nanoplate-enhanced chemiluminescence and macromolecular shielding for rapid microbial diagnostics. *Adv. Healthcare Mater.* **2018**, *7*, 1701506.

(15) Iranifam, M. Analytical applications of chemiluminescence methods for cancer detection and therapy. *TrAC, Trends Anal. Chem.* **2014**, *59*, 156−183.

(16) Yang, X.; Yu, Y.-Q.; Peng, L.-Z.; Lei, Y.-M.; Chai, Y.-Q.; Yuan, R.; Zhuo, Y. Strong Electrochemiluminescence from MOF accelerator enriched quantum dots for enhanced sensing of trace cTnI. *Anal. Chem.* **2018**, *90*, 3995−4002.

(17) Wang, X.; Cui, Q.; Yao, C.; Li, S.; Zhang, P.; Sun, H.; Lv, F.; Liu, L.; Li, L.; Wang, S. Conjugated polyelectrolyte-silver nanostructure pair for detection and killing of bacteria. *Adv. Mater. Technol.* **2017**, *2*, 1700033.

(18) Kang, T.; Li, F.; Baik, S.; Shao, W.; Ling, D.; Hyeon, T. Surface design of magnetic nanoparticles for stimuli-responsive cancer imaging and therapy. *Biomaterials* **2017**, *136*, 98−114.

(19) Hatakeyama, H. Recent advances in endogenous and exogenous stimuli-responsive nanocarriers for drug delivery and therapeutics. *Chem. Pharm. Bull.* **2017**, *65*, 612−617.

(20) Lu, C.-H.; Willner, I. Stimuli-responsive DNA-functionalized nano-/microcontainers for switchable and controlled release. *Angew. Chem., Int. Ed.* **2015**, *54*, 12212−12235.

(21) Shu, Y.; Song, R.; Zheng, A.; Huang, J.; Chen, M.; Wang, J. Thermo/pH dual-stimuli-responsive drug delivery for chemo-/photothermal therapy monitored by cell imaging. *Talanta* **2018**, *181*, 278−285.

(22) Karimi, S.; Heydari, M. Voltammetric mixture analysis of tyrosine and tryptophan using carbon paste electrode modified by newly synthesized mesoporous silica nanoparticles and clustering of variable-partial least square: Efficient strategy for template extraction in mesoporous silica nanoparticle synthesis. *Sens. Actuators, B* **2018**, *257*, 1134−1142.

(23) Wang, Z.; Yang, X.; Yang, J.; Jiang, Y.; He, N. Peroxidase-like activity of mesoporous silica encapsulated Pt nanoparticle and its application in colorimetric immunoassay. *Anal. Chim. Acta* **2015**, *862*, 53−63.

(24) Bartosova, Z.; Krejci, L. Nucleases in homologous recombination as targets for cancer therapy. *FEBS Lett.* **2014**, *588*, 2446−2456.

(25) Oroval, M.; Climent, E.; Coll, C.; Eritja, R.; Aviñó, A.; Marcos, M. D.; Sancenón, F.; Martínez-Máñez, R.; Amorós, P. An aptamer-

DOI: 10.1021/acssensors.9b01303
ACS Sens. 2019, 4, 2922−2929

gated silica mesoporous material for thrombin detection. *Chem. Commun.* **2013**, *49*, 5480−5482.
(26) Chen, C.; Pu, F.; Huang, Z.; Liu, Z.; Ren, J.; Qu, X. Stimuli-responsive controlled-release system using quadruplex DNA-capped silica nanocontainers. *Nucleic Acids Res.* **2011**, *39*, 1638−1644.
(27) Pascual, L.; Cerqueira-Coutinho, C.; García-Fernández, A.; de Luis, B.; Bernardes, E. S.; Albernaz, M. S.; Missailidis, S.; Martínez-Máñez, R.; Santos-Oliveira, R.; Orzaez, M.; Sancenón, F. MUC1 aptamer-capped mesoporous silica nanoparticles for controlled drug delivery and radio-imaging applications. *Nanomed. Nanotechnol. Biol. Med.* **2017**, *13*, 2495−2505.
(28) Marino, D. D. Water and food safety in the developing world: global Implications for health and nutrition of infants and young Children. *J. Am. Diet. Assoc.* **2007**, *107*, 1930−1934.

DOI: 10.1021/acssensors.9b01303
ACS Sens. 2019, 4, 2922−2929